

Role of network dynamics in shaping spike timing reliability

Maxim Bazhenov,¹ Nikolai F. Rulkov,^{2,3} Jean-Marc Fellous,⁴ and Igor Timofeev⁵

¹*Salk Institute, 10010 North Torrey Pines Road, La Jolla, California 92037, USA*

²*Institute for Nonlinear Science, University of California, San Diego, La Jolla, California 92093-0402, USA*

³*Information Systems Laboratories, Inc., San Diego, California 92121, USA*

⁴*Department of Biomedical Engineering and Center for Cognitive Neuroscience, Duke University, Durham, North Carolina 27708, USA*

⁵*Laval University, Quebec, Canada G1K 7P4*

(Received 12 November 2004; revised manuscript received 22 April 2005; published 5 October 2005)

We study the reliability of cortical neuron responses to periodically modulated synaptic stimuli. Simple map-based models of two different types of cortical neurons are constructed to replicate the intrinsic resonances of reliability found in experimental data and to explore the effects of those resonance properties on collective behavior in a cortical network model containing excitatory and inhibitory cells. We show that network interactions can enhance the frequency range of reliable responses and that the latter can be controlled by the strength of synaptic connections. The underlying dynamical mechanisms of reliability enhancement are discussed.

DOI: [10.1103/PhysRevE.72.041903](https://doi.org/10.1103/PhysRevE.72.041903)

PACS number(s): 87.18.Sn, 05.45.Xt, 84.35.+i

Cortical neurons display complex intrinsic resonance properties that are produced and controlled by the particular set of intrinsic membrane conductances and that may vary with the type of neurons [1]. The intrinsic neuronal resonances influence the spike timing reliability (STR) and, thus, affect information processing. Experimental studies of synaptically isolated cortical pyramidal cells and interneurons *in vitro* have shown that such reliability of firing, when driven by a sinusoidal stimulus, has an optimal frequency range that depends on the amplitude of the stimulus, and on the type of neuron studied [2]. *In vivo*, this single cell resonance phenomenon may explain a variety of electroencephalographic (EEG) data related to many network-level cortical rhythms [3,4]. These rhythms appear during different behavioral states: slow oscillations with strong delta rhythms (0.5–2 Hz) are associated with deep sleep [4], oscillations dominated by theta frequencies (4–12 Hz) are related to cognitive processing and cortico-hippocampal interactions [5], and gamma oscillations (30–80 Hz) are often found in the cortex and other brain structures under attentive behavioral conditions [6].

The questions we address in this study are the following. (i) How does the intrinsic frequency dependence of STR change when neurons are synaptically coupled to form a cortical network? (ii) What is the possible role of synaptic interconnections in the control of STR? To allow for large-scale network simulations, we use the recently introduced map-based models of cortical neurons [7]. These models are shown to replicate the resonance properties of cortical neurons found *in vitro* and are designed to capture the dynamical mechanisms underlying the generation of various types of spiking activity [7].

The model of a regular spiking (RS) neuron that represents a cortical pyramidal cell can be written as follows [8]:

$$x_{n+1} = f_{\alpha}(x_n, x_{n-1}, y_n + \beta_n),$$

$$y_{n+1} = y_n - \mu(x_n + 1) + \mu\sigma + \mu\sigma_n, \quad (1)$$

where x_n and y_n are the fast and slow dynamical variables, respectively, $\mu \ll 1$, and $f_{\alpha}(\dots)$ is a piecewise nonlinear function. The function is designed to shape spiking oscillations in fast subsystems and contains three intervals which can be written as follows:

$$f(x_n, x_{n-1}, u) = \begin{cases} \alpha/(1-x_n) + u & \text{if } x_n \leq 0 \\ \alpha + u & \text{if } 0 < x_n < \alpha + u \text{ and } x_{n-1} \leq 0 \\ -1 & \text{if } x_n \geq \alpha + u \text{ or } x_{n-1} > 0, \end{cases} \quad (2)$$

where u stands for the third argument related to the corresponding slow subsystem and input variable.

The input variables β_n and σ_n introduce the action of synaptic current, I^{syn} , and other currents injected into the neuron. The individual dynamics of the model (no input currents: $\beta_n=0$ and $\sigma_n=0$) as functions of control parameters σ and α are discussed elsewhere [8,9]. The input variables of (1) are proportional to the injected current I_n , namely $\beta_n = \beta^e I_n$ and $\sigma_n = \sigma^e I_n$.

The parameters of model (1) can be tuned to replicate the firing patterns of a typical RS neuron when it spikes in response to a rectangular depolarizing current pulse I_n [7]. The parameters were set to the values $\alpha=3.65$, $\sigma=0.06$, $\mu=0.0005$, $\beta^e=0.133$, and $\sigma^e=1$. This model replicates the effects of spike-frequency adaptation (deceleration of spiking) and spike after-hyperpolarization. The time constants of these effects are controlled by the value of the parameter μ .

Model for fast spiking (FS) interneuron. The typical firing patterns of FS interneurons in response to a rectangular pulse do not exhibit the spike adaptation observed in pyramidal cells, but show noticeable after-hyperpolarization caused by each generated spike. To capture the hyperpolarization effect, the slow subsystem in the model (1) was substituted by the equation for a phenomenological hyperpolarizing current I_n^{hp}

generated by the action of each spike as follows [7]:

$$I_{n+1}^{\text{hp}} = \gamma^{\text{hp}} I_n^{\text{hp}} - \begin{cases} g^{\text{hp}} & \text{if } x_n \text{ is at the top of a spike} \\ 0 & \text{otherwise.} \end{cases} \quad (3)$$

The parameter γ^{hp} controls the duration, $\tau^{\text{hp}} \sim (1 - \gamma^{\text{hp}})^{-1}$, and the parameter g^{hp} controls the amplitude of the hyperpolarization current. The model of the FS neuron in this case can be written in the following form:

$$x_{n+1} = f_\alpha(x_n, x_{n-1}, y^{\text{rs}} + \beta^{\text{hp}} I_n^{\text{hp}} + \beta^e I_n), \quad (4)$$

where y^{rs} is a constant defining the resting state of the model, and I_n^{hp} is the new slow variable computed above with (3). The parameter values of the FS interneuron model were set as follows [7]: $\alpha = 3.8$, $y^{\text{rs}} = -2.9$, $\beta^{\text{hp}} = 0.5$, $\gamma^{\text{hp}} = 0.6$, $g^{\text{hp}} = 0.1$, and $\beta^e = 0.1$.

Modeling of synaptic interconnections. In the map-based models, we use conventional ordinary differential equation models of synaptic currents rewritten in the form of difference equations. The simplest equation for a synaptic current can be written as

$$I_{n+1}^{\text{syn}} = \gamma I_n^{\text{syn}} - g_{\text{syn}} \times \begin{cases} x_n^{\text{post}} - x_{\text{rp}}, & \text{spike}_{\text{pre}}, \\ 0 & \text{otherwise,} \end{cases} \quad (5)$$

where g_{syn} is the strength of synaptic coupling, and the indexes “pre” and “post” stand for the presynaptic and postsynaptic variables, respectively. The first condition, “spike_{pre},” is satisfied when $x_n^{\text{pre}} \geq \alpha + y_n^{\text{pre}} + \beta_n^{\text{pre}}$ or $x_{n-1}^{\text{pre}} > 0$, i.e., when the value x_n^{pre} is in the rightmost interval of the function (2). It corresponds to the times of presynaptic spikes. Parameter γ in (5) controls the relaxation rate of the synaptic current after the presynaptic spike is received ($0 \leq \gamma < 1$). The parameter x_{rp} defines the reversal potential and, therefore, the type of synapse: excitatory or inhibitory.

Frequency dependence of spike timing reliability. The dependence of the STR on the frequency of somatically injected sinusoidal currents was studied experimentally in [2]. In this study, we focus on the analysis of STR when each cell receives synaptic stimuli in the form of Poisson distributed spike trains with periodically modulated mean rate: $r(n) = f_c [1 - \sin(2\pi f_m n \tau)]$, where $f_c = 200$ Hz, $\tau = 0.5$ ms is the sampling period, n is the discrete time (iteration), and f_m is the frequency of periodic modulation. We studied the spiking responses as a function of f_m in the range of 0–30 Hz and different strengths of synaptic inputs.

The results of the *in vitro* experiments and the simulations obtained for the case of RS neurons are shown in Fig. 1. The experiments were carried out using coronal slices of rat prefrontal and infralimbic areas of the prefrontal cortex. The coronal slices were obtained from 2–4-week-old Sprague-Dawley rats. Rats were anesthetized with Isoflurane (Abbott Laboratories, IL) and decapitated. Their brains were removed and cut into 350- μm -thick slices using standard techniques. Patch-clamp was performed under visual control at 30–32 °C. Synaptic transmission was blocked by D-2-amino-5-phosphonovaleric acid (D-APV; 50 μM), 6,7-dinitroquinoxaline-2,3, dione (DNQX; 10 μM), and bicuculline methiodide (bic; 20 μM). All drugs were obtained from RBI or Sigma, freshly prepared in ACSF and bath ap-

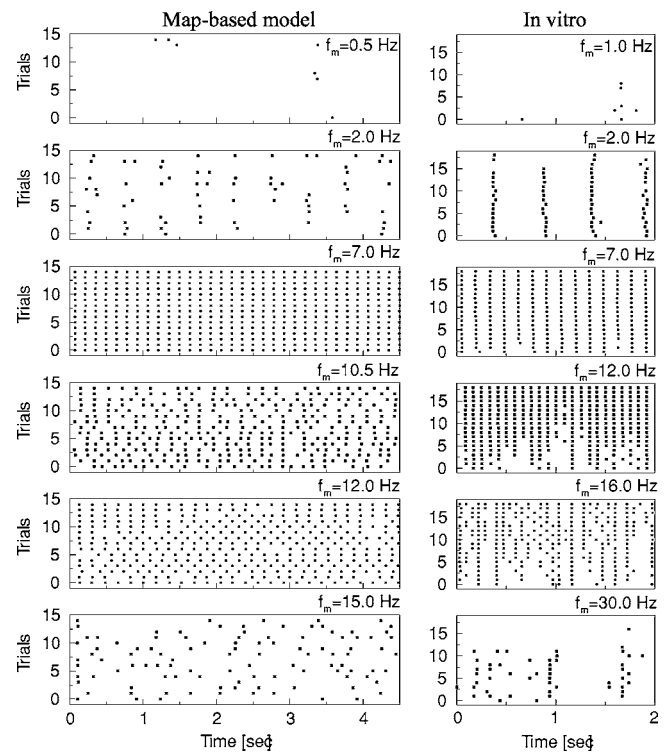


FIG. 1. Spiking of RS neuron in response to frequency modulated Poisson-type inputs plotted for 16 trials and six different modulation frequencies f_m . Map-based model of RS cell (left) and experiment with a RS cell of a rat prefrontal cortex (right). Synaptic inputs: $g = 0.0003$, $\gamma = 0.875$.

plied. Whole cell patch-clamp recordings were achieved using glass electrodes (4–10 M Ω containing mM: KmeSO₄, 140; Hepes, 10; NaCl, 4; EGTA, 0.1; Mg-ATP, 4; Mg-GTP, 0.3; Phosphocreatine 14). Data were acquired in current clamp mode using an Axoclamp 2A amplifier (Axon Instruments, Foster City, CA). Data acquisition rate was 10 kHz. All *in vitro* experiments were carried out in accordance with animal protocols approved by the Salk Institute.

In the model simulations, the RS neuron received 100 sine-wave modulated excitatory synaptic stimuli with synaptic strength $g_{\text{syn}} = 0.0003$ and synaptic time constant $\gamma = 0.875$. The amplitude of the periodic input modulation was selected such that a neuron remained silent for a constant input of maximal amplitude. For low modulation frequencies, both *in vitro* and modeled neurons produced spikes at only a few input maxima, making the reproducibility of spike trains from one trial to another low (see top panels in Fig. 1). As the input modulation frequency increased, the reliability of spiking improved. At about 7 Hz, both *in vitro* and modeled neurons displayed almost perfect one-to-one locking with the input modulation. In the model, the initial increase of responsiveness with the input speedup at low-frequency modulation may be better understood if we consider that the change of variables $z_n = y_n + \beta_n$, $\beta_n = \beta^e I_n$ in model (1) eliminates external current from the first equation but adds its first derivative ($I_{n+1} - I_n$) to the second one. Increasing the frequency of modulation increases the amplitude of the input current derivative and, therefore, increases the

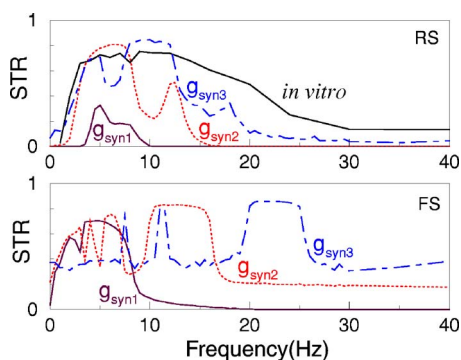


FIG. 2. (Color online) Frequency dependence of STR in map-based model. The reliability of responses in synaptically isolated RS (top panel) and FS (bottom panel) cells. Different curves correspond to three different stimulation amplitudes ($g_{\text{syn}1}=0.00018$, $g_{\text{syn}2}=0.0003$, $g_{\text{syn}3}=0.00055$); synaptic time constant $\gamma=0.875$. Upper solid line in the top panel corresponds to the RS cell of a rat prefrontal cortex. STR *in vitro* was calculated from 19 independent trials.

drive to the system even though the amplitude of the input remains constant. In the range of moderate frequencies (3–13 Hz), the modulation elicits subthreshold oscillations close to the spike threshold and the neurons demonstrate the resonant properties. For very high frequencies, the reproducibility of spike trains was reduced again, reflecting the inability of both *in vitro* and modeled neurons to follow high-frequency inputs (see bottom panel in Fig. 1). To quantify the reproducibility of spike trains, the spike-timing reliability (STR) \mathcal{R} of a cell computed for N responses to the stimuli can be evaluated as follows [1]:

$$\mathcal{R} = \frac{1}{N^2} \sum_{i=1}^N \sum_{j=1, j \neq i}^N \frac{\sum_{n=1}^L u_i(n) u_j(n)}{\sqrt{\sum_{n=1}^L u_i^2(n) \sum_{n=1}^L u_j^2(n)}}, \quad (6)$$

where L is the length of the trace (stimulus) and $u_i(n) = s_i(n) * G(n)$ is the convolution of a Gaussian function $G(n) = \exp[-n^2/(2w^2)]$ and the i th spike train computed from the corresponding response pattern x_n with the following algorithm: $s_i(n)=1$ if the n th iteration of x_n results in a spike, and $s_i(n)=0$ if it does not. The width of $G(n)$ at the level of half-amplitude was set to 20 ms ($w=8.5$). This width was chosen to match the time scale at which the analyses are done (single spikes precision). Spike triggered averages show that the membrane potential is different from baseline up to about 5–10 ms around a spike on average, so the Gaussian width should be in this same range. We also varied the width of the Gaussian window to study its effect on the resonance curve. When w was reduced to $w=5$ (half-amplitude width is 12 ms), the peaks of the resonance curves became lower and narrower. Increase of w to $w=10$ (half-amplitude width is 23.5 ms) had an opposite effect. In both cases, however, all the main features of the resonance curves shown in Fig. 2 were well preserved. Choosing an even larger width of the Gaussian window could make it comparable with the time scale of bursts, therefore overshadowing the individual spike precision.

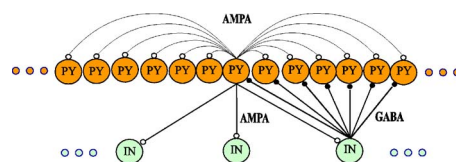


FIG. 3. (Color online) Structure of synaptic coupling in a population of neurons. AMPA, excitatory synapses; GABA, inhibitory synapses.

The change of STR as a function of frequency has one or more “humps” caused by the intrinsic resonance properties of the cell. The origin of the resonance is the subthreshold oscillations observed in the real neurons [2] and captured by the dynamics of the map-based model, see [9] for details. When the amplitude of the input is small, STR reaches its maximum values in the 5–7 Hz range (see Fig. 2). As the amplitude of the stimulus increases, this range shifts to frequencies higher than 10 Hz. Thus, the model correctly captures the shift of reliability resonance when the strength of the input synapses increases, mimicking the experimental data when the amplitude of the injected current is increased [2]. Figure 2 also shows the humps of STR associated with resonance of cells on double frequency of the modulation (when the cell periodically fails to produce a spike at the peaks of the stimuli) and on subharmonics [when it produces several spikes (a burst) for each period of modulation]. The reliability curve calculated for layer 5 RS cell of rat prefrontal cortex (upper curve in Fig. 2) has a wide resonance peak and is best matched by the model-based $g_{\text{syn}3}$ curve. It lacks the fine structure found in the model, which could be attributed to the relatively large response variations from one trial to another *in vitro* (e.g., because of nonstationarity of the baseline membrane potential).

The map-based model of the FS neuron does not have the subthreshold oscillations as in the RS cell model, but the recovery process from the spike after-hyperpolarization and subthreshold dynamics of the fast map (4) set the characteristic time scale; this time scale defines the range of frequencies for which the reliability of FS neuron responses increases significantly. This time scale changes with the depolarization level. This causes the shift of reliability humps produced by the increase in synaptic input shown in Fig. 2 (bottom panel).

Spike timing reliability in the network. Lateral excitatory connections between pyramidal cells (RS type) and feedback/feedforward inhibition mediated by cortical interneurons (FS type) affect the STR of the population response. To study the effects of network interactions, we simulated a two-layer two-dimensional network model of 256 excitatory pyramidal (PY) neurons and 64 inhibitory interneurons (INs). The radius of connection fan-out was eight neurons (200 presynaptic neurons) for AMPA mediated PY-PY synapses; eight (200 presynaptic neurons) neurons for AMPA mediated PY-IN synapses; two (12 presynaptic neurons) neurons for GABA_A mediated IN-PY synapses. A one-dimensional sketch of this network is shown in Fig. 3. STR was calculated for each PY neuron using $N=10$ input trials and averaged over all PY neurons in the network. Each cell in the network received 100 external excitatory synaptic

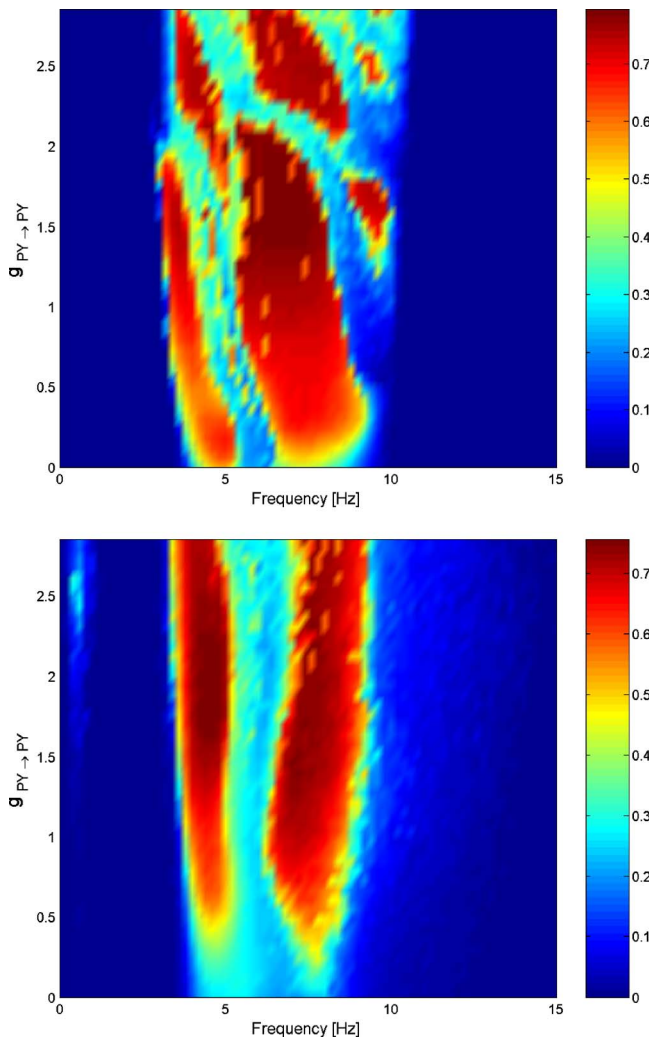


FIG. 4. (Color online) Frequency dependence of STR in the network model with different strength of excitatory coupling. Top panel, the network without inhibitory feedback ($g_{IN \rightarrow PY}=0$); bottom panel, the network with inhibitory feedback ($g_{IN \rightarrow PY}=1.5$ is the maximal conductance that could be activated by all inhibitory synapses projected to a single PY cell). $\gamma=0.9$ for inhibitory synapses and $\gamma=0.875$ for excitatory synapses. The values of STR are indicated in the bars shown at the right hand side of the plots.

stimuli with synaptic strengths $g_{syn}=0.00018$ and time constants $\tau=0.875$. The results of the simulations are shown in Figs. 4 and 5.

We found that the influence of synaptic coupling was most prominent for low stimulation amplitudes. An isolated PY neuron would skip spikes under weak stimulus conditions even at the optimal stimulation frequency, and the reliability remained low (see g_{syn1} in Fig. 2). However, placing neurons in the network by including the excitatory coupling between PY neurons increased the probability of firing for all neurons; a PY neuron firing first initiated an immediate spread of activity over the whole network. In a population of N neurons, the probability to find at least one spike for each input maximum increases linearly with N , therefore network responsiveness improves significantly for large N (Fig. 4, top). Without inhibitory feedback (i.e., $g_{IN \rightarrow PY}=0$), however,

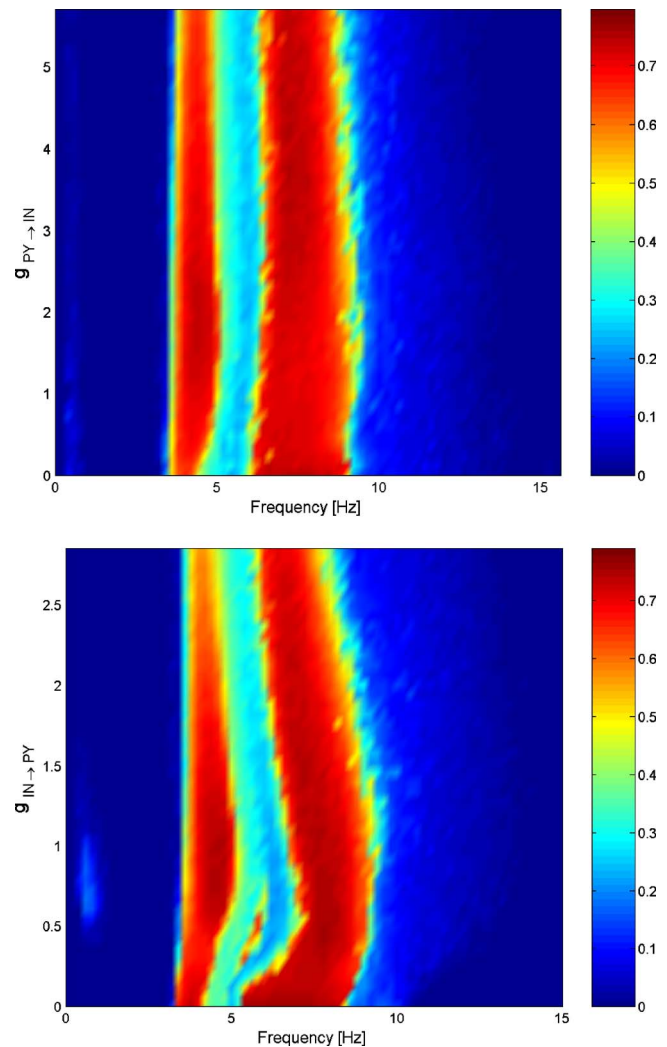


FIG. 5. (Color online) Frequency dependence of STR in the network model as a function of inhibitory feedback. The top panel shows the variation of the excitatory (AMPA-mediated) input from pyramidal cells to the inhibitory interneurons. The bottom panel shows that the increase of the inhibitory input from interneurons sharpened the reliability curve and shifted its peaks. $g_{PY \rightarrow PY}=1.5$. The values of STR are indicated in the bars shown at the right hand side of the plots.

the increase of excitation created a bursting regime with spike bursts at each peak of the external input modulation. The timing of the spikes within each burst fluctuated significantly and led to the unsteady variations of the STR-frequency dependence as the value of $g_{PY \rightarrow PY}$ varied (Fig. 4, top). We tested if these variations may be a result of the limited number of trials used to calculate STR and found that the positions and relative sizes of all STR peaks remained unchanged when the number of trials varied. Increase of $g_{PY \rightarrow PY}$ excitation increases the number of spikes produced on top of each sine wave modulation peak, therefore changing the STR. The inhibitory feedback reduced the variability of the STR (Fig. 4, bottom). The inhibitory postsynaptic potentials mediated by fast-spiking interneurons provided a feedback inhibition that terminated the burst after its first spike.

Figure 5 shows that the STR changed significantly as inhibitory feedback increases from zero. As soon as inhibition became sufficient to limit PY responses to the single spike events, the shape of STR curve stabilized and further increases of inhibition produced only minor changes to the width of the STR humps. Note that the exact position of the reliability peaks in the frequency domain continued to change, indicating that the strength of synaptic coupling in the network controls its response properties. Change of PY \rightarrow IN or IN \rightarrow PY coupling produced similar effects, however the shifts of the reliability peaks were more noticeable when the inhibition was modified directly (IN \rightarrow PY conductance).

Our results suggest that excitatory connections between PY neurons in the network promote increased sensitivity through spreading excitation, while the inhibitory feedback increases the reliability by balancing the excitation level. These mechanisms help the network of neurons to create an operating mode during which even weak inputs can be transmitted with high precision through oligosynaptic chains. The network dynamics can therefore reshape the resonance properties of the neurons and significantly enhance their reliability when processing weak stimuli.

In many sensory systems, the mean firing rate of neurons contains information about the stimulus [10]. For downstream neurons to read this information efficiently, the integration window of a neuron should exceed the average interspike interval. If the biological system utilizes this coding strategy, the bursts of spikes (rather than individual spikes) become units of neural information [11]. However, in various biological systems a different strategy seems to be used; the neurons act as coincidence detectors integrating their input over short periods, therefore responding selectively to corre-

lated input [12]. The selectivity for coincident inputs has been linked to different intrinsic and circuit properties. Recent studies suggest that coincidence detection allows an olfactory system to discriminate between similar odors and to improve the reliability of the system against uncorrelated noise in its input [13]. In this earlier study, we showed that the response of a neuron with a small enough integration window (coincidence detector) depended critically on the reliability and synchrony of spiking across presynaptic units. Our new study suggests that the biological networks can be “tuned” to specific frequencies; stimuli at these frequencies will induce reliable and synchronous responses in the population of neurons. Postsynaptic (downstream) cells operating as coincidence detectors would then respond selectively to these inputs and would remain silent when different “nonpreferred” inputs are presented. Therefore, instead of relaying all the inputs to the downstream levels, a network of excitatory and inhibitory neurons such as shown in Fig. 3 may selectively augment some inputs and inhibit others. Since different groups of neurons within a network may possess different resonance properties, our study suggests a mechanism capable of “routing” specific inputs to their desirable synaptic targets. Changing the intrinsic and synaptic properties of the network modifies its resonance frequencies, and, thus, can control the information flow as well as its processing.

ACKNOWLEDGMENTS

This research was supported by grants from NIDCD (M.B.) and the Canadian Institutes of Health Research (I.T.). The authors are grateful to T.J. Sejnowski and E. Ohayon for stimulating discussions.

-
- [1] S. Schreiber, J.-M. Fellous, P. H. E. Tiesinga, and T. J. Sejnowski, *J. Neurophysiol.* **91**, 194 (2004).
 - [2] J.-M. Fellous, A. R. Houweling, R. H. Modi, R. P. N. Rao, P. H. E. Tiesinga, and T. J. Sejnowski, *J. Neurophysiol.* **85**, 1782 (2001).
 - [3] C. Basar-Eroglu, E. Basar, T. Demiralp, and M. Schurmann, *Int. J. Psychophysiol.* **13**, 161 (1992); P. Achermann and A. A. Borbely, *Neuroscience* **85**, 1195 (1998); A. Glass and R. J. Riding, *Biol. Psychol.* **51**, 23 (1999).
 - [4] M. Steriade, A. Nunez, and F. Amzica, *J. Neurosci.* **13**, 3266 (1993).
 - [5] O. S. Vinogradova, *Prog. Neurobiol.* **45**, 523 (1995).
 - [6] W. Singer and C. M. Gray, *Annu. Rev. Neurosci.* **18**, 555 (1995); R. Ritz and T. J. Sejnowski, *Curr. Opin. Neurobiol.* **7**, 536 (1997); P. Fries, J. H. Reynolds, A. E. Rorie, and R. Desimone, *Science* **291**, 1560 (2001).
 - [7] N. F. Rulkov, I. Timofeev, and M. Bazhenov, *J. Comput. Neurosci.* **17**, 203 (2004).
 - [8] N. F. Rulkov, *Phys. Rev. E* **65**, 041922 (2002).
 - [9] A. L. Shilnikov and N. F. Rulkov, *Int. J. Bifurcation Chaos Appl. Sci. Eng.* **13**, 3325 (2003).
 - [10] D. H. Hubel and T. N. Wiesel, *J. Physiol. (London)* **160**, 106 (1962); K. H. Britten, M. N. Shadlen, W. T. Newsome, and J. A. Movshon, *J. Neurosci.* **12**, 4745 (1992); A. J. Parker and W. T. Newsome, *Annu. Rev. Neurosci.* **21**, 227 (1998).
 - [11] J. E. Lisman, *Trends Neurosci.* **20**, 38 (1997).
 - [12] M. Abeles, *Isr. J. Med. Sci.* **18**, 83 (1982); C. E. Carr and M. Konishi, *J. Neurosci.* **10**, 3227 (1990); W. R. Softky and C. Koch, *ibid.* **13**, 334 (1993); P. Konig, A. K. Engel, and W. Singer, *Trends Neurosci.* **19**, 130 (1996); J. Perez-Orive, O. Mazor, G. C. Turner, S. Cassenaer, R. I. Wilson, and G. Laurent, *Science* **297**, 359 (2002).
 - [13] J. Perez-Orive, M. Bazhenov, and G. Laurent, *J. Neurosci.* **24**, 6037 (2004).